Vol. 44, No. 4 (2022) 687-695, DOI: 10.24874/ti.1312.05.22.09

Tribology in Industry

www.tribology.rs

RESEARCH

Effect of SiO_2 and B_4C Nanoparticles Hybrid Addition on Mechanical Properties of AA6061-T6 Surface Composite via Friction Stir Processing

Mohammed S. Ali[a,*] and Iman Q. Al Saffar[a]

[a]*Mechanical Engineering Department, College of Engineering, University of Baghdad, Baghdad, Iraq.*

Keywords:

Aluminum alloys
Friction stir processing
SiO_2
B_4C
Hybrid nanoparticles
Composite

* Corresponding author:

Mohammed S. Ali
E-mail:
mohammed.ali2003m@coeng.uobaghdad.edu.iq

Received: 29 May 2022
Revised: 19 July 2022
Accepted: 10 September 2022

A B S T R A C T

This paper studies the effect of SiO_2 and B_4C nanoparticles on the mechanical properties (microhardness, wear resistance, and tensile strength) of an aluminum alloy 6061-T6 composite. The friction stir process was used to generate a composite surface layer by incorporating Nano-sized SiO_2 and B_4C nanoparticles as a hybrid addition into the AA6061-T6 alloy at the best rotational speed of (1200) rpm, (30) mm/min travel speed, 3 mm hole depth, and an equal amount of SiO_2 and B_4C (7.5) wt.% for each nanoparticle. Samples were examined microstructurally using optical and Field Emission Scanning Electron Microscopy. Adding SiO_2 and B_4C nanoparticles as a hybrid addition to AA6061-T6 gives a superior improvement in the hardness (155) HV as compared to the parent material (65) HV. The wear test showed that the wear type was oxidative or mild at (5 N) low load and became metallic or severe wear when loading was increased to (15 N) for a sliding time of 20 minutes.

1. INTRODUCTION

Because of its light weight, strength, and corrosion resistance, the aluminum alloy AA6061-T6 is utilized widely in aerospace and marine vehicles and defines applications. In many applications, however, this alloy has poor tribological properties [1]. In comparison to the base metal (unreinforced alloy), the Al alloy (ceramic-phase reinforcement composite matrix) showed superior hardness, good resistance to wear, and improved high-temperature characteristics compared to the conventional alloys [2].

FSP has a wide range of applications, including (a) ultrafine grain formation in superplastic Al alloys [6,10–12], (b) agglomerated Al nanoparticles homogenization [13], (c) Al composite fabrication [14-16], and (d) surface composite fabrication [14-16]. Freshly-generated composites are Al matrix composites (AMCs) created by reinforcing aluminum alloy with nanoparticles such as B_4C, SiO_2, and Ti.

These composites have superior properties to base alloys, such as stiffness, hardness, and wear resistance [3]. The distribution of micro and nanoparticles on the Al alloy surface, as well as their reinforcement, is difficult to achieve using typical surface modification procedures [4]. Surface composites are also made using laser-beam and thermal-spraying processes, but these compromise the properties, leading to the generation of undesired phases. Friction stir processing (FSP) may be the best way to prepare surface composites or surfaces for modification. When such issues are taken into account, this is a relatively new operation performed in solid state technology, which is a version of the friction stir welding (FSW) process that was developed at the Welding Institute (TWI) in 1991 [5]. A no consumed revolving tool with a shoulder and pin is inserted into a base metal plate and designed to traverse in a defined path of friction stir line. Surface composites are also made using laser-beam and thermal-spraying processes, but these compromise the properties, leading to the generation of undesired phases. Due to heat generated by friction between the revolving tool and workpiece, the base metal softens and plasticizes. The capability to add second phase nanoparticles in the stir zone (SZ) and generate a surface composite is thus given by the material blending action and the thermomechanical properties of the process.

Muna K. Abbass et al. (2020) investigated the influence of SiC micro-size particles on the microhardness and resistance to wear of an Al alloy fabricated via FSP, AA6061-T6. To generate a particulate composite surface layer (FSP) was employed to mix micro-sized particles of SiC into the 6061-T6 Al alloy. When compared to the FSPed sample without nanoparticles, adding SiC microparticles to 6061-T6 increased microhardness and wear resistance by 62.6 percent. At low loads (5 N), the wear resistance was mild or oxidative but increased to metallic or severe wear at greater loads (20 N) for a 20-minute sliding time [1].

In 2016, Kishan et al. examined the effect of Nano-sized particle volume percentage on the behavior of tribological, microstructural, and mechanical properties of 6061-T6 aluminum alloy reinforced with nanoparticles produced by friction stir processing. They discovered that increasing the volume percentage of TiB_2 nanoparticles improved hardness as compared to the base metal [8]. (2017) investigated the influence of adding (Al_2O) nanoparticles on the mechanical properties of an AA6061-T6 alloy surface composite using FSP. They observed that adding ceramic particles to the matrix material tends to increase microhardness and wear resistance but decreases yielding strength. Al/SiC composites had a lower friction coefficient than Al/Al_2O_3 composites. As the nanoparticle volume percentage increased in the metal matrix, the nanoparticle reinforcement's effect on the resistance to wear also increased.

T.S. Kumar et al. (2020) used FSP to fabricate Al6061/ZrC composite. To reinforce three different ZrC volume fractions (3, 6, and 9 percent) in the matrix, three different groove widths were created. The composite was processed with a tool rotating at 1200 rpm and a traverse speed of 30 mm/min. A microhardness tester was used to test the composite materials' microhardness. The pin-on-disc tribometer was used to evaluate the composite's sliding wear behavior, and the worn-out surfaces were inspected to identify the wear mechanisms. Results revealed that upon grain refinement, uniform dispersion, and stronger bonding, the addition of ZrC particles increased microhardness. With an increase in the volume fraction of the reinforcing particles, the wear resistance has risen. [17]

Essam B. Moustafa et al. (2022) investigate the effect of adding mono-nanoparticles and niobium carbide (NbC) and tantalum carbide (TaC) hybrids on the microstructural, mechanical, and electrical, of AA2024 using FSP. Polarized optical microscopy examination, showed that the grain was refined and equiaxed, whereas SEM and XRD analyses showed a good distribution of nanoparticles in the metal matrix. In comparison to the base alloy, the mechanical characteristics of the hybrid AA2024/TaC NbC nanocomposites improved by around 15.2, 16.7, and 20.6 percent, respectively, the ultimate compressive stress. A maximum value of 73 percent was achieved in comparison to the basic alloy because of how the hybrid nanocomposites' hardness behavior changed dramatically with aging time [21].

Sampath Boopathi et al. (2022) investigate the effect of B_4C particles volume percentage on the tensile strength and wear resistance of AA2024 to design and predict the maximum tensile strength and minimum wear rate, Taguchi technique was used. SEM, EDS, and XRD analyses were conducted to examine the microstructure of the composite surface. Results showed that the optimum FSP parameters were, 900 rpm rotational speed, 60 mm/min liner speed, and 15% B_4C volume. The maximum tensile strength was 650 MPa and the minimum wear rate was 1.2 mm^3/Nm [22].

Shahin Arshadi Rastabi et al. (2022) study the effect of adding Mg particles and the number of passes on the microstructure and tensile strength of AA1050. They found that the increase in the number of passes lead to decreasing in the grain size in the stir zone and an increase in the heat-affected zone in addition to a more uniform distribution of Al-Mg in the matrix, whereas the addition of Mg particles resulted in considerable grain refinement. Results showed that the tensile strength increased with the increase of passes number until four passes [23].

2. EXPERIMENTAL WORK

A plate of AA6061-T6 aluminum alloy was used in this investigation. A cutting machine was used to prepare this plate to a dimension of 5*100*200 mm. The chemical analysis of this alloy was evaluated using a spectrometer analyzer instrument as shown in Table 1, while Table 2 shows the mechanical characteristics of the alloy AA6061-T6.

Table 1. Chemical composition for used alloy AA6061-T6 compared with the standard.

Elements	Si	Cu	Mg	Cr
Standard	0.7 max	0.4 max	1.2 max	0.35 max
Measured value	0.38	0.07	1.2	0.21
Elements	Ni	Ti	Fe	Zn
Standard	0.5 max	0.15 max	0.8 max	0.25 max
Measured value	0.001	0.03	0.30	0.11
Elements	Mn	Other	Al	
Standard	0.15 max	0.8 max	Bal.	
Measured value	0.80	0.20	Bal.	

T6: Solution heat treatment and artificial aging.

Table 2. Mechanical properties of 6061-T6 Al alloy.

Al Alloy AA6061-T6	YS MPa	TS MPa	El. %	Hardness Kg/mm2
Measured value	148	200	8.35	65
Standard value *	275	311	12	94

* Datasheet for ASM Aerospace Specification Metals Inc.

A vertical type CNC milling machine (MARUFUKU Japan) was used to perform the friction stir processing. As shown in Figure 1, the specimens were first prepared, and then they were fixed firmly using fabricated fixtures designed especially for this process, to ensure that the plates were firmly in place and not removed by friction forces. The tool was employed in the work pace designated region. As illustrated in Figure 2, a non-consumable cylindrical shoulder with a threaded pin manufactured of high-speed steel (HSS) with a 20 mm shoulder diameter, and 6 mm pin diameter, and a length of 3 mm was used, with a tool tilt angle of 2.5°, which is similar to that used in reference [1].

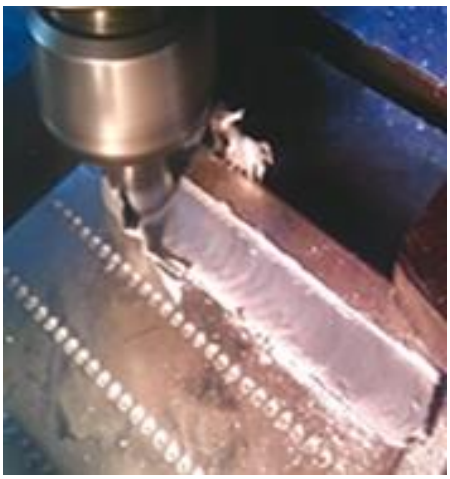

Fig. 1. Specimen during friction stir process.

Fig. 2. Shoulder with threaded pin.

After fixing the plate, several holes were drilled in the spaceman's center for adding SiO_2 and B_4C nanoparticles in three different SiO_2/B_4C ratio concentration mixtures (1/1, 1/2, and 1/3). Which is equivalent to (15%, 15.3%, and 15.5) wt. % respectively according to the following equation.

$$m = \frac{mi}{mtot} \cdot 100\% \quad (1)$$

Where:

m = mass fraction

mi = mass of reinforcement

m_{tot} = the total mass of the processed region and the reinforcement material [11].

The space between holes is 2 mm. The holes have a diameter of 3 mm and three different depths (2, 2.5, and 3) mm. 40 holes were made using the CNC milling machine mentioned above.

The process was conducted by the rotation of the tool in a clockwise direction. The spindle rotated automatically at its plug for 15 seconds (dwelling time) to preheat before the process until the tool's shoulder penetrated the surface of the plate by 0.2 mm. FSP was carried out at a rotational speed of 1200 rpm and a traverse speed of 30 mm/min which represent the best result.

SiO_2 nanoparticles' average size was 25 nm, whereas for B_4C it was 60 nm. Firstly, the holes are filled with nanoparticles. The reinforced volume according to a new technique which was used by Muna and Noor Alhuda [1], the reinforcing volume Fraction for the FSP composite was set at 10%, and then a shoulder without pin was used to close the holes to keep the nanoparticles inside during the process. The total volume friction of drilled holes produced in a plate subjected to friction stir processing, as well as the nanoparticle density, determined the volume fraction (10 vol.%), which can be calculated by dividing the volume of the reinforcement material by the total volume of the processed region of nanoparticles added in this study [11]. The rotating tool was employed on the sample surface to a depth specified at 3.3 mm, which corresponds to the layer thickness of FSP.

3. RESULTS AND DISCUSSION

3.1 Microhardness and microstructure inspection

The samples were collected from the cross-section of the friction stir processing, and then the microstructure was examined using scanning electron microscopy SEM. The Vickers hardness test was used to determine the microhardness profiles over SZ by applying a load of 200 g for a duration of 15 sec. in the direction of FSP. A pin-on-disk was used to conduct the wear tests, changing the applied load for all samples at a fixed time and speed of sliding under the dry sliding condition. Change loads of 5, 10, and 15N, with a sliding time of 15 minutes and a distance of 5 cm at a constant sliding speed of (490) rpm.

3.2. Microstructure results

The microstructural specimens were taken from a cross-section of FSP at 1200 rpm and 30 mm/min, 3 mm hole depth, and 1/1 SiO_2/B_4C ratio are illustrated in Figure 3 (a, b).

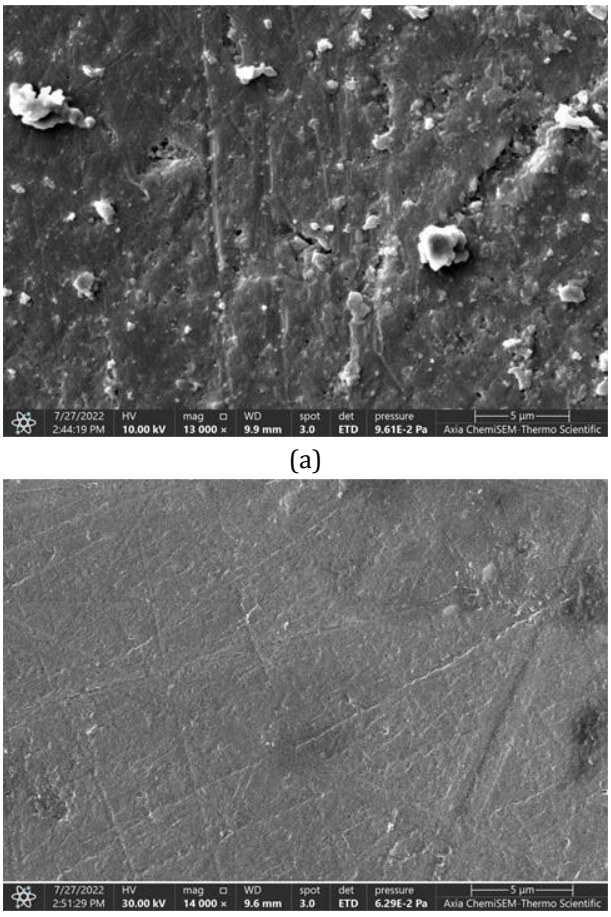

(a)

(b)

Fig. 3. Samples microstructure, (a) Base alloy, (b) Samples after (FSP).

The FSPed sample has four distinct zones, the stir zone (SZ) is a region that is processed thermomechanically with ultra-fine grain size and homogenous structure, the friction stir processed zone (FSPZ), the thermomechanical affected zone (TMAZ), that has an elongated grain since it was deformed thermomechanically, and the heat affected zone (HAZ), that has the same grain-size and structure as the base metal (BM), which is considered as an unaffected region by the process. Figure 4 indicates four zones with varied microstructure properties in the friction stir process, reinforced by nanoparticles: a-stir zone (SZ), b-composite material zone (CMZ), and c-heat affected zone (HAZ), and d-thermomechanically affected zone (TMAZ) as can be seen.

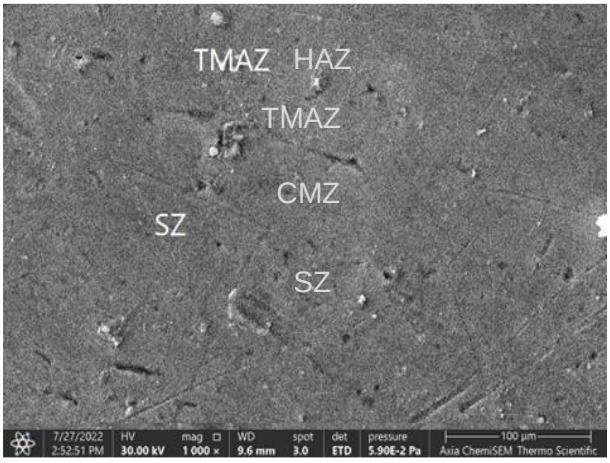

Fig. 4. Specimen reinforced by nanoparticles microstructures.

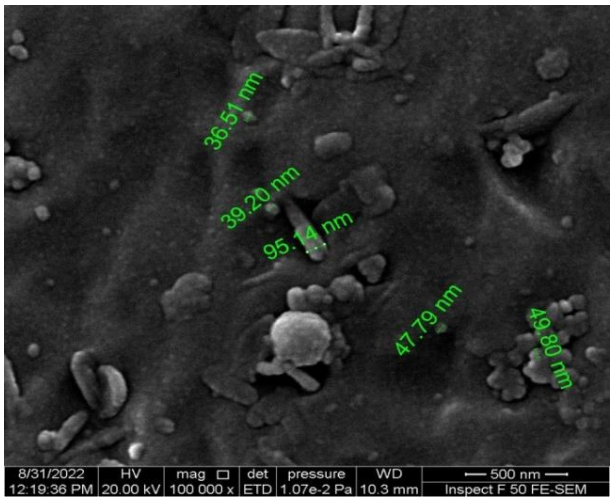

Fig. 5. FESEM analysis of composite samples microstructures clarifies the reinforcement distribution in SZ.

As illustrated in Figure 5, the nanoparticles are more uniformly distributed in the thermo-mechanically affected zone and the stir zone. This is because the rotating tool generates sufficient heat and circumferential force for nanoparticles to be dispersed over a larger area. Some nanoparticle groups are prompted at SZ, the particles' distribution in the aluminium metallic matrix, due to the metal flow type in the SZ during the process.

3.3 Fesem mapping and EDS analysis

The sample microstructure that FSP produced at 1200 rpm and 30 mm/min, 3 mm hole depth, and reinforced with equal amounts of SiO_2 and B_4C has a smooth and more uniformly grain-structure as visualized by the SEM mapping as shown in Figure 6.

The use of friction stir processing improved the mechanical properties of the treated alloy when compared to the base metal. During the FSP, the grains recrystallized due to a combination of strong plastic, deformation, and contact with a high temperature in the treatment zone. Figure 6 shows the FESEM micrograph of the reinforced specimen with SiO_2 and B_4C nanoparticles, as determined by EDS analysis in Figure 7. In addition, nanoparticles of SiO_2 and B_4C are present in the Al matrix in different regions of the stir zone of the friction stir processing samples in the form of elements Mg, Al, and Si. The regularity of the structure and the characteristics of AA6061-T6 were improved by adding these nanoparticles.

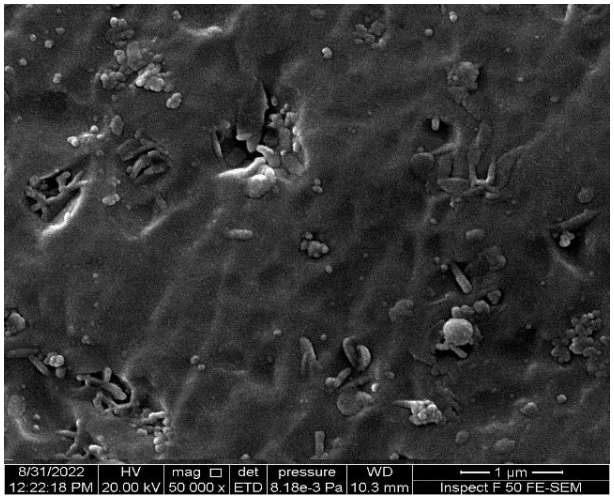

Fig. 6. FESEM elemental mapping of samples reinforced with nanoparticles.

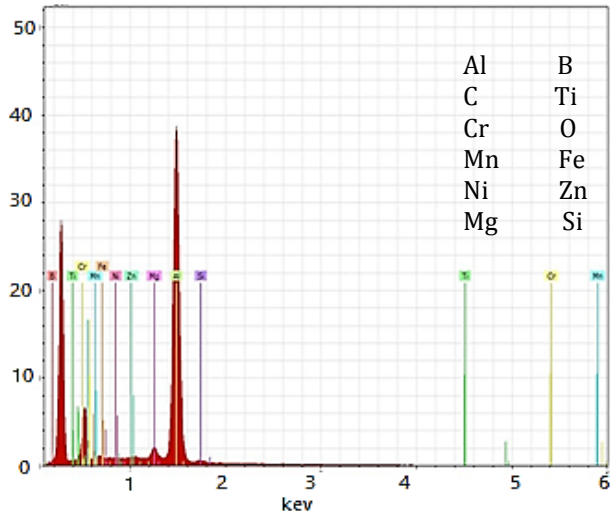

Fig. 7. EDS analysis of samples reinforced with nanoparticles.

3.4 Microhardness

Vickers microhardness distribution through a cross-section of FSPed samples is depicted in figure 8. The distribution of microhardness of the friction stir processed samples were measured on a cross-section typical of the direction of tool traverse at 1200 rpm rotating speed, 30 mm/min travel speed, 3 mm hole depth, and a 1/1 SiO_2/B_4C ratio.

The hardness of the stir zone was higher than that of the HAZ, TMAZ, and heat unaffected zone. Hardness increased with the nanoparticle addition, as seen in Figure 8.

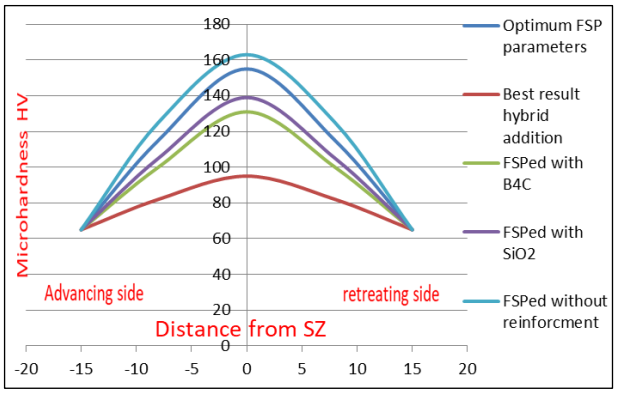

Fig. 8. The distribution of microhardness.

Such results could be attributable to the good microhardness of ceramic nanoparticles and the fine grain structure in the SZ. Due to the refinement of grain and the dynamic-recrystallization of SZ, in addition to the existence of the Al_3Mg_2 phase, the peak hardness in the centre of SZ was 154 HV, as represented by XRD analysis in Figure 9.

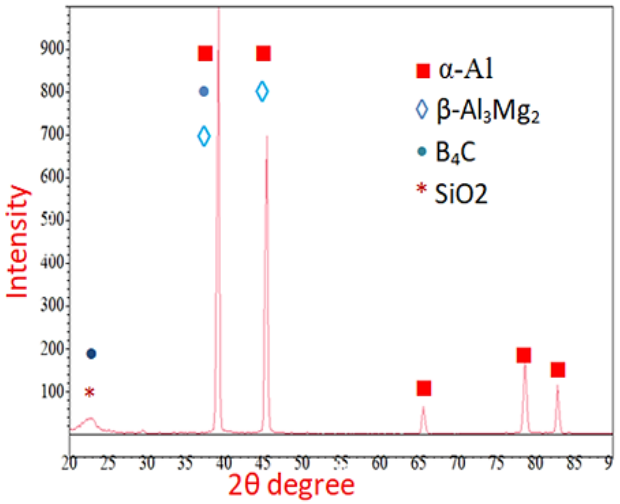

Fig. 9. Analysis of FSPed AA6061-T6 reinforced with nanoparticles.

Figure 8 shows the microhardness characteristics of FSP samples with and without reinforcement in the whole FSP region. The microhardness value in the centre of the surface composite region that was reinforced with nanoparticles was higher than the other composites.

As shown in Table 3, the values of microhardness for (BM), samples that were submitted to FSP only (without adding nanoparticles), samples reinforced with SiO_2, samples reinforced with B_4C, and samples reinforced with hybrid addition of (SiO_2 + B_4C) nanoparticles at different mixing ratio.

Table 3. FSPed samples microhardness at different additions of nanoparticles in SZ.

No.	FS sample	Microhardness g/cm
1	Base metal	65
2	FSPed without any addition	81
3	FSPed with SiO_2 nanoparticle	131
4	FSPed with B_4C nanoparticles	139
5	FSPed with 1/1 (B_4C/SiO_2)	155
6	FSPed with 1/2 (B_4C/SiO_2)	147
7	FSPed with 1/3 (B_4C/SiO_2)	143

Samples after processing without adding nanoparticles achieved a microhardness of (81 HV), the single addition of SiO_2 achieved a microhardness of (131 HV), whereas the single addition of B_4C nanoparticles attained a microhardness of (139 HV), but samples that were reinforced with hybrid addition of (B_4C+SiO_2) nanoparticles in the region of stirring when the mixing ratio of nanoparticles was 1/1,

achieved a peak value of (155 HV) as compared to the base metal, whose microhardness was (65 HV), whereas in the ratio of 1/2 and 1/3 the hardness was (147, 143 HV) respectively, that was due to the good distribution of nanoparticles in the stir zone and the refined grain size of the parent alloy, as well as friction heat and plastic flow during the processing, creating equiaxed fine grains that are recrystallized dynamically in the stir zone. The decrease in grain-size increases yield strength and thus the value of hardness, depending on the Hall-Petch relationship.

Figure 10 shows the error bars chart for microhardness of samples reinforced with a different mixing ratio of B_4C/SiO_2 in addition to the base material and of B_4C and SiO_2 nanoparticles.

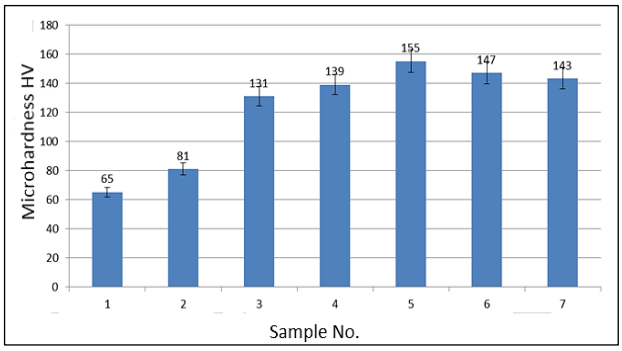

Fig. 10. Error bars chart for microhardness.

3.5 Results of wear test

The wear rate was determined using the weight loss method for both parent metal and FSP samples, which were treated at(1200 rpm) speed of rotation, 30 mm/min traverse speed, hole depth of 3 mm, and an equal amount of SiO_2 and 4CB. The behavior of Al-alloy composites which were reinforced by nanoparticles was examined at various loads (5, 10, and 15 N) for 20 min. and a 490 rpm sliding speed. The rate of wear tends to increase as the loads' increase in constant time and speed of sliding. As shown in figure 11, the wear behaviour is equal for all specimens.

Figure 11 also depicts 3 wear regions: mild, transition, and severe wear. Under 10 N load, the behavior of wear changes from a mild to a severe wear type. The rate of wear of the FSP samples was lower than that of the base material. Due to the presence of fine grains in FSP samples compared to the unprocessed Al alloy AA6061-T6, as a result of dynamically severe plastic deformation and recrystallization.

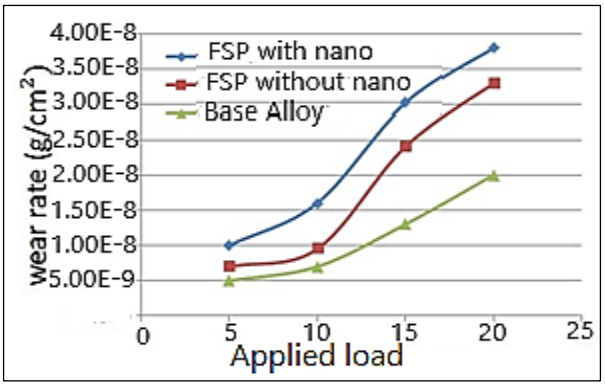

Fig. 11. The Effects of applying loads on the rate of wear resistance.

4. CONCLUSIONS

This research studies the effect of hybrid addition of B_4C and SiO_2 nanoparticles on the mechanical properties and wears behavior of AA6061-T6 under the best conditions for FSP.

Results showed that the hybrid addition of SiO_2 and B_4C nanoparticles to AA6061-T6 aluminum alloy enhanced mechanical properties such as microhardness and wear resistance. This was due to the very fine grain size obtained after friction stir processing and the homogenized distribution of nanoparticles on the surface of the alloy. Other observations were:

1. The best conditions for FSP were noticed at 1200 rpm rotation speed, 30 mm/min traverse speed, 3 mm hole depth, and a 1/1 SiO_2/B_4C ratio.
2. It was observed that the stir zone SZ had the peak microhardness, which was decreased further away to the thermo-mechanical affected region and heat affected region, then towards the base metal 6061-T6 alloy for spaceman after processing.
3. The addition of SiO_2 and B_4C nanoparticles to 6061-T6 Al alloy improves the wear resistance as well as microhardness compared to the parent metal.
4. Wear rate increases with increasing applied load (5 to 15 N) at a constant sliding time (15) min. and sliding speed of (490 rpm) for composites and base metal.
5. Results showed better wear resistance and microhardness for reinforced samples with nanoparticles of SiO_2 and B_4C than the parent material 6061-T6 and samples that were submitted to FSP without nanoparticles.

REFERENCES

[1] M.K., Abbas, N.A., Baheer, *Effect of SiC Particles on Microstructure and Wear Behaviour of Fabricated by Friction Stir Processing*, in 3rd International Conference on Engineering Sciences, 4–6 November, 2019, Kerbala, Iraq, doi: 10.1088/1757-899X/671/1/012159

[2] R. Bauri, D. Yadav, G. Suhas, *Effect of friction stir processing (FSP) on microstructure and properties of Al–TiC in situ composites*, Materials Science and Engineering: A, vol. 528, iss. 13-14, pp. 4732–4739, 2011, doi: 10.1016/j.msea.2011.02.085

[3] M. Nagaral, B. Auradi, *Effect of Al2O3 Particles on Mechanical and Wear Properties of 6061al Alloy Metal Matrix Composites*, Journal of Material Sciences & Engineering, vol. 2, iss. 1, pp. 1-4, 2013, doi: 10.4172/2169-0022.1000120

[4] M.K. Abbassa, N.A.B. Sharhan, *Optimization of Friction Stir Processing Parameters for Aluminium Alloy (AA6061-T6) Using Taguchi Method*, Al-Qadisiyah Journal for Engineering Sciences, vol. 12, no. 1, pp. 1–6, 2019 doi: 10.30772/qjes.v12i1.580

[5] R.S. Mishra, Z.Y. Ma, *Friction stir welding and processing*, Material Sciences and Engineering, vol. 50, iss. 1-2, pp. 1-78, 2005, doi: 10.1016/j.mser.2005.07.001

[6] P.B. Berbon, W.H. Bingel, R..S. Mishra, C.C. Bampton, M.W. Mahoney, *Friction stir processing: a tool to homogenize nanocomposite aluminum alloys*, Scripta Materialia, vol. 44, iss. 1, pp. 61-66, 2001, doi: 10.1016/S1359-6462(00)00578-9

[7] V. Kishan, A. Devaraju, K.P. Lakshmi, *Influence of volume percentage of NanoTiB2 particles on tribological and mechanical behaviour of 6061- T6 Al alloy nano-surface composite layer prepared via friction stir process*, Defence Technology, vol. 13, iss. 1, pp. 16-21, 2017, doi: 10.1016/j.dt.2016.11.002

[8] S. Rathee, S. Maheshwari, A. Noor Siddiquee, M. Srivastava, *Effect of tool plunge depth on reinforcement particles distribution in surface composite fabrication via friction stir processing*, Defense Technology, vol. 13, Iss. 2, pp. 86-91, 2017, doi: 10.1016/j.dt.2016.11.003

[9] N. Yuvaraj, S. Aravindan, Vipin, Fabrication of Al5083/B4C surface composite by friction stir processing and its tribological characterization, Journal of Materials Research and Technology, vol. 4, iss. 4, pp. 398–410, 2015, doi: 10.1016/j.jmrt.2015.02.006

[10] E. Moustafa, *Effect of Multi-Pass Friction Stir Processing on Mechanical Properties for AA2024/Al2O3 Nanocomposites*, Materials, vol. 10, iss. 9, pp. 1–17, 2017 doi: 10.3390/ma10091053

[11] A.D Mc. Naught, A. Wilkinson, *Compendium of Chemical Terminology,* International Union of Pure and Applied Chemistry, 1997.

[12] I. Sudhakar, V. Madhu, G.M. Reddy, K.S. Rao, *Enhancement of wear and ballistic resistance of armour grade AA7075 aluminium alloy using friction stir processing*, Defense Technology, vol. 11, iss. 1, pp. 10-17 2015 doi: 10.1016/j.dt.2014.08.003

[13] M.K. Abbass, K.M. Raheef, *Effect of welding parameters on mechanical properties of friction stir lap welded joints for similar aluminium alloys (AA1100-H112 and AA6061-T6)*, Journal of Engineering and Sustainable Development, vol. 22, no. 3, pp. 60-71, 2018.

[14] M.K. Abbass, H.H. Abd, *A Comparison Study of Mechanical Properties between Friction Stir Welding and TIG Welded Joints of Aluminium Alloy (Al 6061-T6)*, Eng. & Tech. Journal, vol. 31, no. 1, pp. 2701-2715, 2013.

[15] M.K. Abbass, *Laser Surface Treatment and Modification of Aluminium Alloy Matrix Composites*, Lasers in Manufacturing and Materials Processing, vol. 5, iss. 1, pp. 81- 94, 2018, doi: 10.1007/s40516-018-0054-6

[16] M.K. Abbass, M.J. Fouad, *Study of Wear Behaviour of Aluminium Alloy Matrix Nano composites Fabricated by Powder Technology*, Eng. & Tech. Journal, vol. 32, pp. 1720-1732, 2014.

[17] T.S. Kumar, R. Raghu, S. Shalini, *Hardness and Wear Behavior of Al 6061/ZrC Composite Processed by Friction Stir Processing*, Tribology in industry, vol. 42, no. 4, pp 582-591, 2020 doi: 10.24874/ti.855.02.20.10

[18] N. Parumandla, K. Adpeu, *Effect of Al2O3 and SiC Nano Reinforcements on Microstructure, Mechanical and Wear Properties of Surface Nanocomposites Fabricated by Friction Stir Processing*, Material Science, vol. 24, no. 3. pp. 1392–1320, 2018, doi: 10.5755/j01.ms.24.3.18220

[19] R. Bauri, D. Yadav, *Metal Matrix Composites by Friction Stir Processing*, Elsevier, 2018, doi: 10.1016/C2016-0-04019-6

[20] K.M. Raheef, *Characteristics of Friction Stir Lap Welding of Dissimilar Ferrous and Non-Ferrous Alloys by New Technique*, PhD thesis, Department of production Engineering and Metallurgy, University of Technology, Baghdad, Iraq, 2018.

[21] E.B. Moustafa, A.H. Elsheikh, M.A. Taha, *The effect of TaC and NbC hybrid and mono-nanoparticles on AA2024 nanocomposite: Microstructure, strengthening, and artificial aging*, Nanotechnology Reviews, vol. 11, no. 1, pp. 2513–2525, 2022 doi: 10.1515/ntrev-2022-0144

[22] S. Boopathi, V.H. Balaji, M. Mageswari, M.M. Asif, *Influences of boron carbide particles on the wear rate and tensile strength of AA2014 surface composite fabricated by friction-stir processing*, Materials and Technology, vol. 56, no. 3, pp. 263–270, 2022, doi: 10.17222/mit.2022.409

[23] S.A. Rastabi, M. Mosallaee, *Effects Of multi pass friction stir processing and Mg addition on the microstructure and tensile properties of Al 1050 alloys,* International Journal of Minerals, Metallurgy and Materials, vol. 29, pp. 97–107, 2022, doi: 10.1007/s12613-020-2074-4